Molecular Microbiology (2014) 91(6), 1164–1178 ■
doi:10.1111/mmi.12526
First published online 17 February 2014

A touch of glue to complete bacteriophage assembly: the tail-to-head joining protein (THJP) family

Isabelle Auzat,[1]* Isabelle Petitpas,[1] Rudi Lurz,[2] Frank Weise[2†] and Paulo Tavares[1]
[1]*Laboratoire de Virologie Moléculaire et Structurale, Centre de Recherche de Gif, CNRS UPR 3296 and IFR115, 91198 Gif-sur-Yvette, France.*
[2]*Max Planck Institute for Molecular Genetics, Ihnestraße 63-73, D-14195 Berlin, Germany.*

Summary

Bacteriophage SPP1 is a nanomachine built to infect the bacterium *Bacillus subtilis*. The phage particle is composed of an icosahedric capsid, which contains the viral DNA, and a long non-contractile tail. Capsids and tails are produced in infected cells by two distinct morphogenetic pathways. Characterization of the suppressor-sensitive mutant SPP1*sus82* showed that it produces DNA-filled capsids and tails but is unable to assemble complete virions. Its purified tails have a normal length but lack a narrow ring that tapers the tail end found at the tail-to-head interface. The mutant is defective in production of gp17. The gp17 ring is exposed in free tails competent for viral assembly but becomes shielded in the final virion structure. Recombinant gp17 is active in an *in vitro* assay to stick together capsids and tails present in extracts of SPP1*sus82*-infected cells, leading to formation of infectious particles. Gp17 thus plays a fundamental role in the tail-to-head joining reaction, the ultimate step of virus particle assembly. This is the conserved function of gp17 and its structurally related proteins like lambda gpU. This family of proteins can also provide fidelity to termination of the tail tube elongation reaction in a subset of phages including coliphage lambda.

Introduction

Bacterial virus (phage or bacteriophage) assembly is a multi-step process that follows a specific sequence of protein–protein and protein-nucleic acid interactions leading to the formation of the infectious particle. Morphogenesis is initiated by formation of an icosahedral procapsid (or prohead), followed by encapsidation of the viral chromosome and ends with fixation of the connector proteins that form the viral DNA gatekeeper complex (Orlova *et al.*, 2003). Phages can have short tails (*Podoviridae* family) that assemble directly at the capsid vertex through which DNA movements occur (DNA translocating vertex or portal vertex), or long tails that can be contractile (*Myoviridae*) or non-contractile (*Siphoviridae*) (Casjens and Hendrix, 1988). Long tails assemble through a pathway independent of capsid assembly and attach to the connector structure. Both assembly strategies are highly conserved. The large predominance of tailed bacteriophages among bacterial viruses (96%; Ackermann, 2007) is attributed to the tail structure that provides an optimized device for DNA delivery to the bacterial cell cytoplasm. This function requires search and specific recognition of the target cell followed by efficient delivery of viral DNA through the membrane(s) and cell wall to reach the cytoplasm.

Tail assembly in *Siphoviridae* and *Myoviridae* phages starts from the initiator complex, which forms the adsorption device at the tail extremity distal from the phage head (for reviews see Aksyuk and Rossmann, 2011; Davidson *et al.*, 2012). Then, polymerization of the tail tube protein (TTP) is anticipated to occur around the tape measure protein (TMP) to form the helicoidal part of the tail. Binding of tail completion proteins was proposed to stop elongation of the tail tube, as found for gpU of lambda, and to provide an interface for association of the tail with the head (Katsura and Kühl, 1974; 1975a,b; Katsura and Tsugita, 1977).

Bacteriophage SPP1 irreversible adsorption to the Gram-positive host *Bacillus subtilis* is most likely mediated by the structural protein gp21 (Vinga *et al.*, 2012) which forms both the tail tip and the end of the cap structure (Fig. 1A, Goulet *et al.*, 2011; Vinga *et al.*, 2012). The gp21 amino-terminus complexed with gp19.1 forms the cap structure which closes the end of the tail tube. The helical SPP1 tail tube is formed by the TTPs gp17.1 and gp17.1*, at a ratio of about 3:1. They share a common amino-terminus, the latter species arising from a programmed translational frameshift (Fig. 1B; Auzat *et al.*, 2008). The

Accepted 18 January, 2014. *For correspondence. E-mail auzat@vms.cnrs-gif.fr; Tel. (+33) (0)1 69 82 38 60; Fax (+33) (0)1 69 82 43 08. †Present address: Department of Molecular Biology, NMI, Markwiesenstraße 55, D-72770 Reutlingen, Germany.

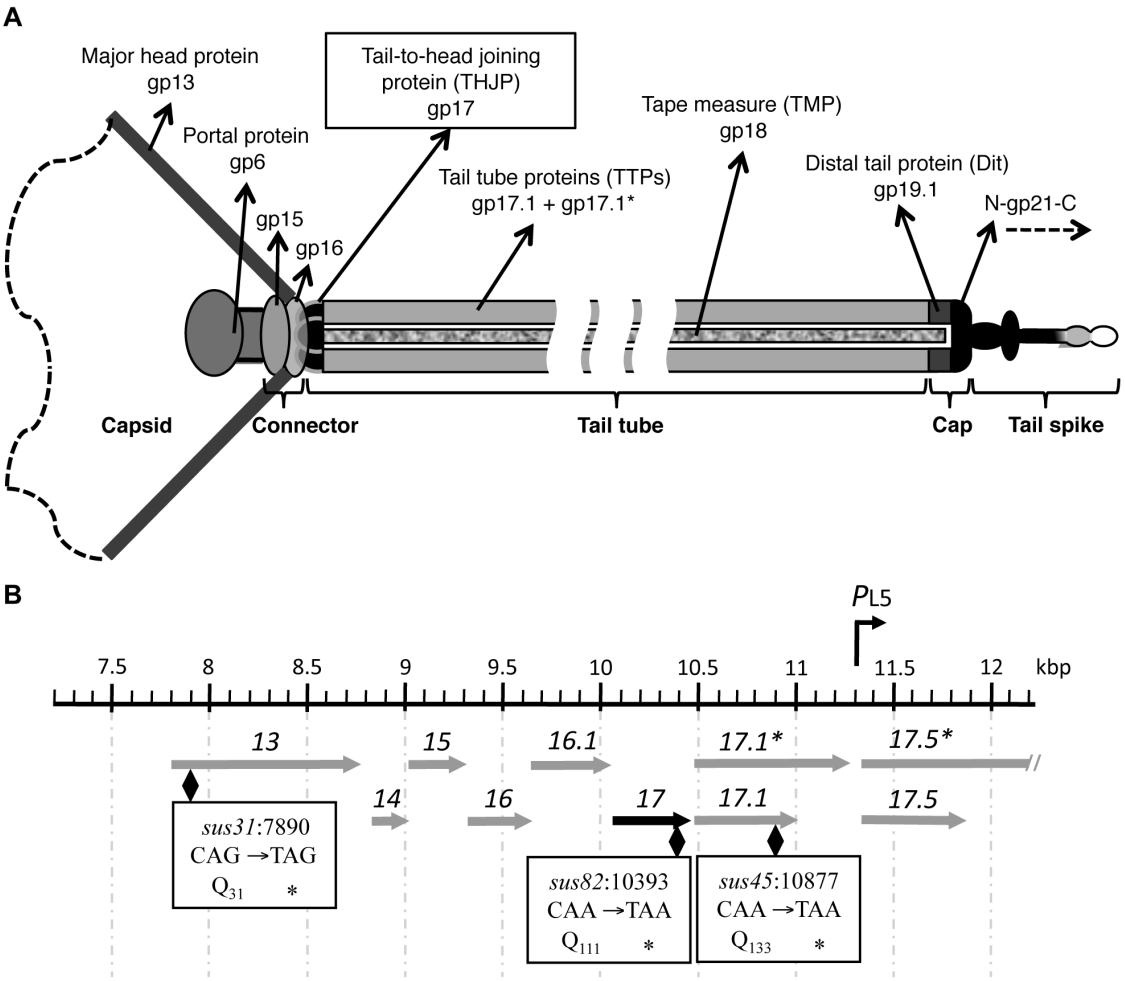

Fig. 1. Schematic representation of the SPP1 phage particle and genetic map of the region surrounding gene *17*.
A. Composition of the phage particle. The grey gradient representing the tail spike denotes the potential presence of yet unidentified proteins (Vinga *et al.*, 2012).
B. Gene organization of the SPP1 genome region encompassing gene *17* which is highlighted in black. The upper ruler shows the genome co-ordinates according to the deposited SPP1 sequence (accession code X97918.2). The SPP1*sus31,* SPP1*sus82* and SPP1*sus45* mutations within genes *13*, *17* and *17.1*, respectively, are indicated by a black diamond. The precise position and the nature of the mutation are detailed inside the black rectangles, asterisks indicating stop codons.

organization of gp17.1 and gp17.1* in the tail tube is unknown. Tails composed exclusively of gp17.1 or of gp17.1* are functional and have identical lengths showing that the two TTP forms are exchangeable (Auzat *et al.*, 2008). The TMP gp18 was proposed to be stretched through the entire length of the tail and probably acts as a scaffold for polymerization of the tail tube proteins gp17.1/gp17.1* (Plisson *et al.*, 2007). Gp18 is expected to determine the size of the tail tube as demonstrated for gpH of phage lambda and for gp29 of phage T4 (Katsura and Hendrix, 1984; Abuladze *et al.*, 1994 respectively).

Recently, the three-dimensional structure of the gp17 monomer has been resolved by NMR (Chagot *et al.*, 2012). This has revealed that gp17 is structurally similar to the gpU protein of bacteriophage lambda, to gp15 of bacteriophage T4, and to two other prophage proteins from Gram-negative bacteria, despite their low sequence identity (Pell *et al.*, 2009; Atia-tul-Wahab *et al.*, 2011; Fokine *et al.*, 2013). GpU is defined as a tail terminator protein because it assembles at the top of the tail tube and prevents aberrant lambda tail polymerization (Katsura and Tsugita, 1977).

Here we describe biochemical and functional properties of gp17 protein. Gp17 is shown to be essential for the tail-to-head joining reaction, leading to the formation of infectious particles, but it is neither necessary for proper tail tube assembly nor necessary for tail tube size determination. These properties reveal a mechanism in which tail length determination is uncoupled from tapering of the tail tube.

Results

*The conditional lethal mutant SPP1*sus82 *is defective for tail-to-head joining*

The library of SPP1 conditional lethal mutants (Behrens *et al*., 1979) was screened by EM for phages defective in the tail-to-head joining reaction. Lysates prepared from the non-permissive strain *B. subtilis* YB886 infected with mutant SPP1*sus82* showed the presence of empty capsids, DNA-filled capsids and tails (Fig. 2A). The *sus82* mutation was mapped by marker rescue in gene *17* (data not shown). The mutation was further characterized by sequencing the entire gene *17* of the SPP1*sus82* genome. A single nucleotide substitution was detected changing a CAA triplet to TAA, thus introducing a premature stop codon at the position of the codon for glutamine 111 (position 10393–10395 of the SPP1 nucleotide sequence; access code X97918.2; Fig. 1B). The gp17 protein is thus required for the joining reaction of bacteriophage tails and heads. It is interesting to note that the position of gp17 protein in the phage structure, between the head and tail, correlates with the location of its gene in the SPP1 genome between the head connector genes *15* and *16* and the *17.1/17.1** genes coding for the tail tube proteins (Fig. 1B).

*Morphology and composition of tails assembled in SPP1*sus82 *infection*

Comparison of the composition of purified bacteriophage SPP1 particles and of SPP1*sus9* tailless phage capsids by Western blot showed that gp17 is a structural protein of the virus particle not present in the capsid structure (not shown). Free tails were then purified from lysates of non-permissive infections with SPP1 mutants blocked either in tail-to-head joining (SPP1*sus82*) or in capsid assembly (SPP1*sus31*) to investigate if gp17 stably associates to tail structures (Fig. 1B). Non-permissive infections with mutant SPP1*sus31* which is defective in production of the major capsid protein gp13 lead to accumulation of assembled tails in the host cytoplasm (Fig. 2B, Becker *et al*., 1997; A. Seul, unpublished). Both lysate production and tail purification experiments were performed in parallel in order to be strictly comparable. Large protein complexes were enriched by centrifugation through a sucrose cushion leading to the accumulation of tails (black arrows in Fig. 2A and B) contaminated with long flagella (asterisk) and other unidentified structures (Fig. 2A and B). DNA-filled (filled diamonds) and empty (empty diamonds) capsids were found exclusively in extracts of SPP1*sus82*-infected cells. Flagella were distinguished from tails by their clearly larger diameter and heterogeneous length, due in part to fragmentation due to mechanical stress during sample preparation. Tails were then partially purified by sedimentation through a glycerol gradient. While large contaminating structures were pelleted (Fig. 2C and D), tails were recovered in the middle of the gradient (Figs 2E and F and 3A and B). Tail proteins co-sedimented in the same fractions of the gradient, 4 to 6, supporting that a homogeneous population of tail structures were assembled in the absence or the presence of gp17 alike, in agreement with EM observations (Fig. 2E and F). As expected, gp13 was only found in the pellet of the mutant SPP1*sus82* gradient (Fig. 3A and B, black arrowheads), well separated from the tail fractions. The protein highlighted by a white arrowhead in Fig. 3A that migrates immediately underneath gp13 was identified by mass spectrometry to be contaminating *B. subtilis* flagellin. This very intense band found in the glycerol gradient pellets did not react with anti-SPP1 serum contrary to the species derived from SPP1*sus82* infection, confirming the presence of gp13 exclusively in the latter extract (Fig. 3B). Gp17 was detected exclusively in tails derived from mutant SPP1*sus31* (Fig. 3B). The tails-containing peak fractions of the glycerol gradients were associated with a few contaminants. Fractions 4 to 6 (Fig. 3A) were therefore pooled and fractionated by anion exchange chromatography to obtain very pure samples (Fig. 2G and H). Tails assembled in SPP1*sus82* and SPP1*sus31* infections exhibited an identical chromatographic behaviour eluting between 280 and 320 mM NaCl (not shown). The different purification steps were characterized by Coomassie Blue-stained SDS-PAGE (Fig. 3C) and Western blot (Fig. 3D) using polyclonal antibodies raised against individual known tail proteins.

SPP1*sus82* and SPP1*sus31* tails were pure and homogeneous when observed by EM. No size heterogeneity through purification was detected, including in structures found in the non-fractionated sucrose cushion pellet (Fig. 2A and B and data not shown). The tails also exhibited identical sedimentation behaviour (Fig. 3A and B). The length of purified tails with and without gp17 was similar: 188.0 ± 3.5 nm ($n = 181$) and 183.9 ± 4.6 nm ($n = 130$) respectively. The measures were made from the blob of the tail spike to the top end of the tail tube. Meticulous examination of the tail extremities of the two populations revealed a thin ring with a diameter smaller than the tail tube which covers the tube top in SPP1*sus31* tails (white arrowheads in Fig. 2J). In the absence of gp17, the end of SPP1*sus82* tail tubes distal from the adsorption apparatus are cut sharply above the helical tail tube (black arrowheads in Fig. 2I), and in a few cases show some diffuse heterogeneity, sometimes thickened in a corolla shape (black rectangle in Fig. 2E). The latter feature was best observed at intermediate steps of purification.

Gp17 is localized at the tail end distal from the tail spike

The topology of gp17 in purified tails was investigated by immuno-EM. The position of the antigen was identified by

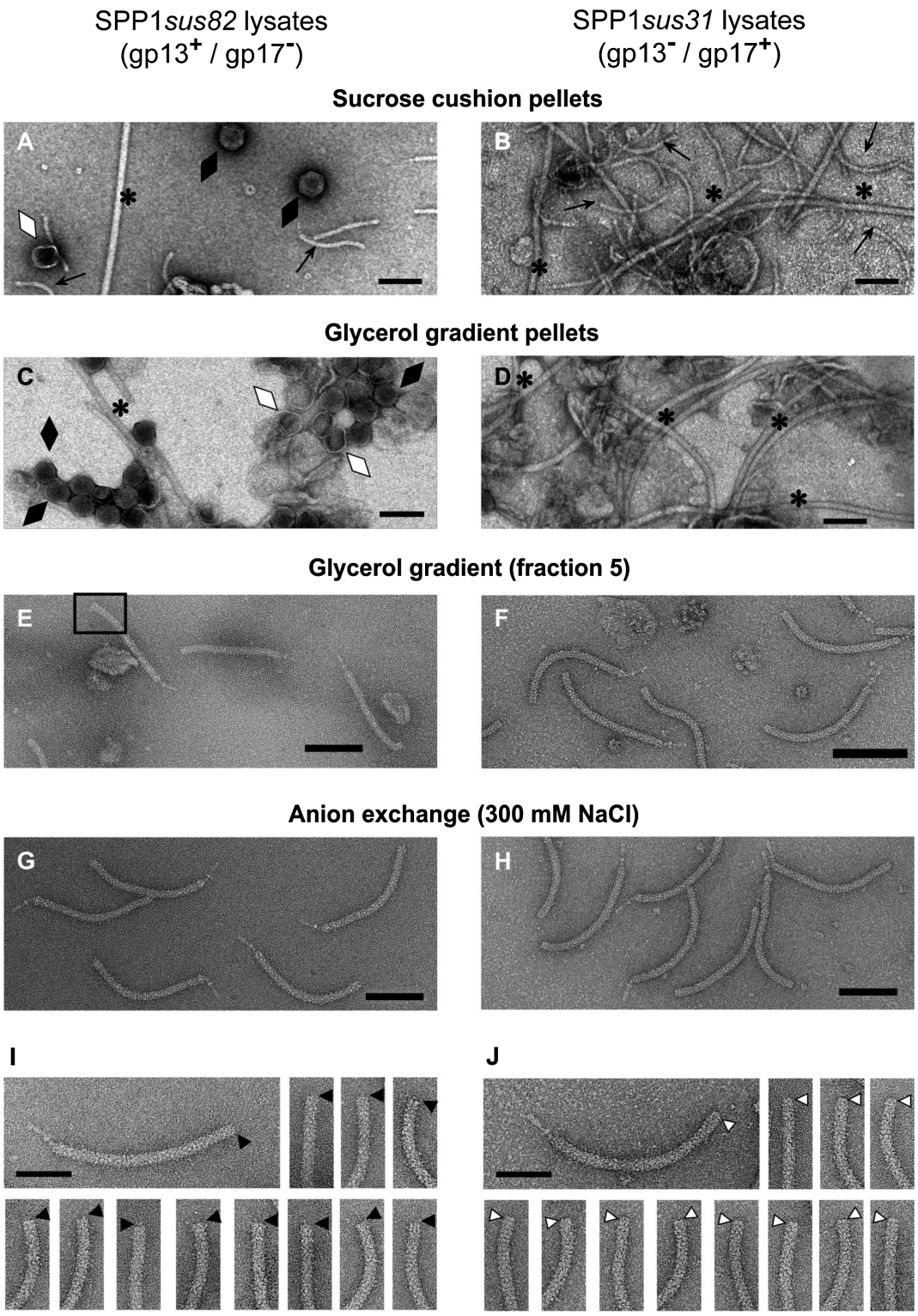

Fig. 2. Tail purification from SPP1*sus82*- and SPP1*sus31*-infected cells monitored by EM. Electron micrographs of *B. subtilis* lysates concentrated by sedimentation through sucrose cushions (A,B), and subsequently fractionated through a 10–30% (w/v) glycerol gradient [pellets (C,D) and fractions 5 enriched in tail structures (E,F)], and after anion exchange chromatography (G,H). The tail end with a corolla shape shown inside the black rectangle in E was sometimes observed in tails derived from SPP1*sus82* infections. Magnifications of the tail end distal from the tail spike highlight absence of the gp17 ring (black arrowheads in I) or its presence (white arrowheads in J) in purified tails. Black diamonds indicate DNA-filled capsids, white diamonds the empty capsids, black arrows the tails and black asterisks the flagella (A–D). The scale bars represent 100 nm in A to H and 50 nm in I and J.

 Molecular Microbiology, **91**, 1164–1178

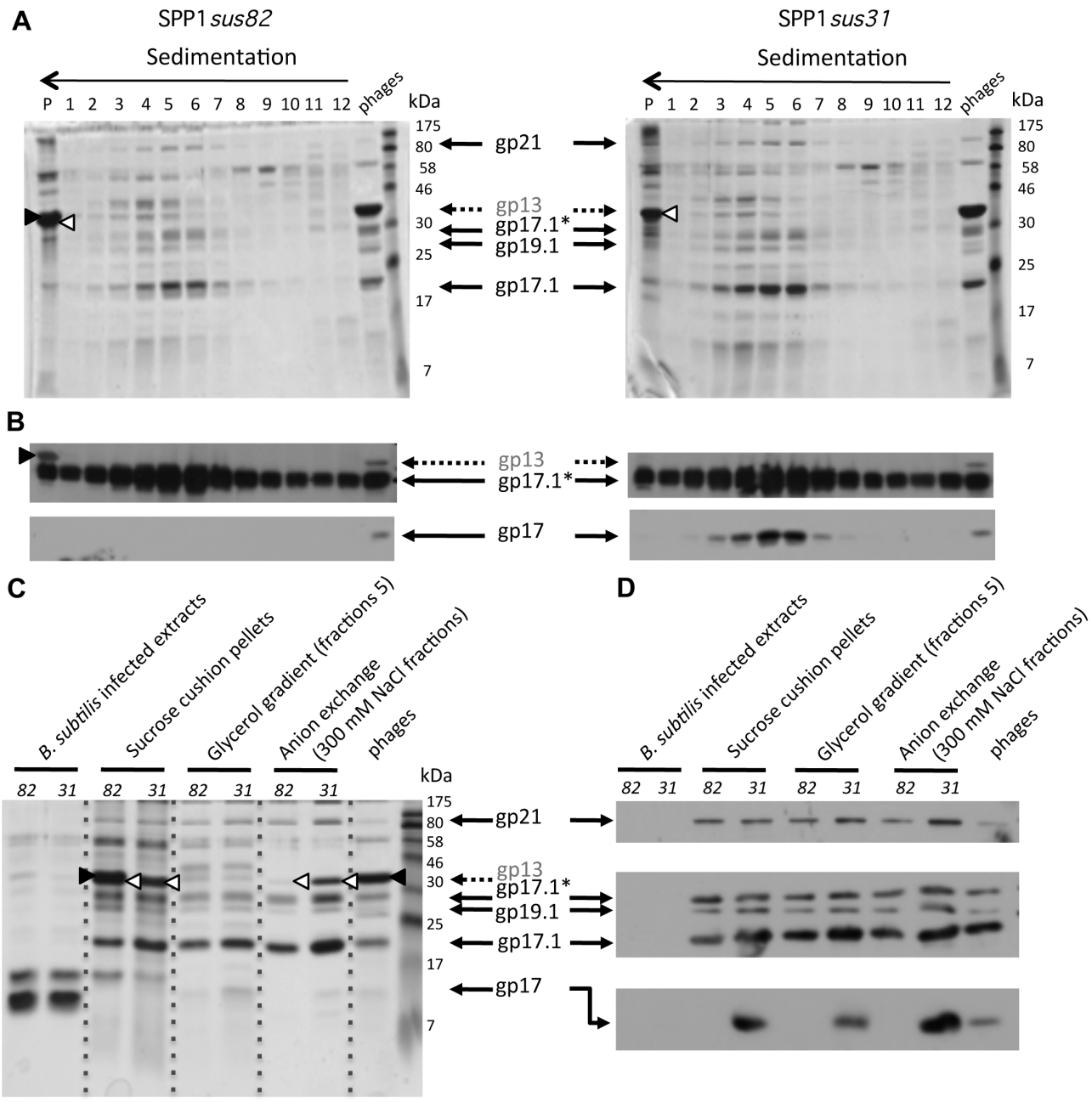

Fig. 3. Tail purification from SPP1*sus82* and SPP1*sus31* lysates monitored by SDS-PAGE (A,C) and by Western blot (B,D).
A and B. Sedimentation profile and composition of tails run through a 10–30% glycerol gradient at 35 000 r.p.m. for 6 h (4°C) followed by fractionation. Fraction numbers are shown above each gel lane (16% SDS-PAGE). P – pellet; 'phages' – purified SPP1 phage particles. Molecular mass standards are presented on the right lane of Coomassie Blue-stained gels (A). Gp17 was detected in Western blots with polyclonal anti-gp17 antibodies while gp13 and gp17.1* were detected with antibodies raised against SPP1 virions (Auzat *et al.*, 2008) (B). The position of SPP1 tail proteins are indicated by black arrows or by a dotted arrow in case of the major capsid protein (gp13). Gp13 and *B. subtilis* flagellin which partially co-migrate in 16% SDS-PAGE are identified in the gels by black and white arrowheads respectively.
C and D. Enrichment of tail structures from extracts of bacteria infected with SPP1*sus82* (lanes *82*) and SPP1*sus31* (lanes *31*) after each step of purification indicated above the gels. Figure labels and methods are as in A and B. Gp19.1 and gp21 were detected with antibodies raised against the purified proteins (Veesler *et al.*, 2010; Vinga *et al.*, 2012).

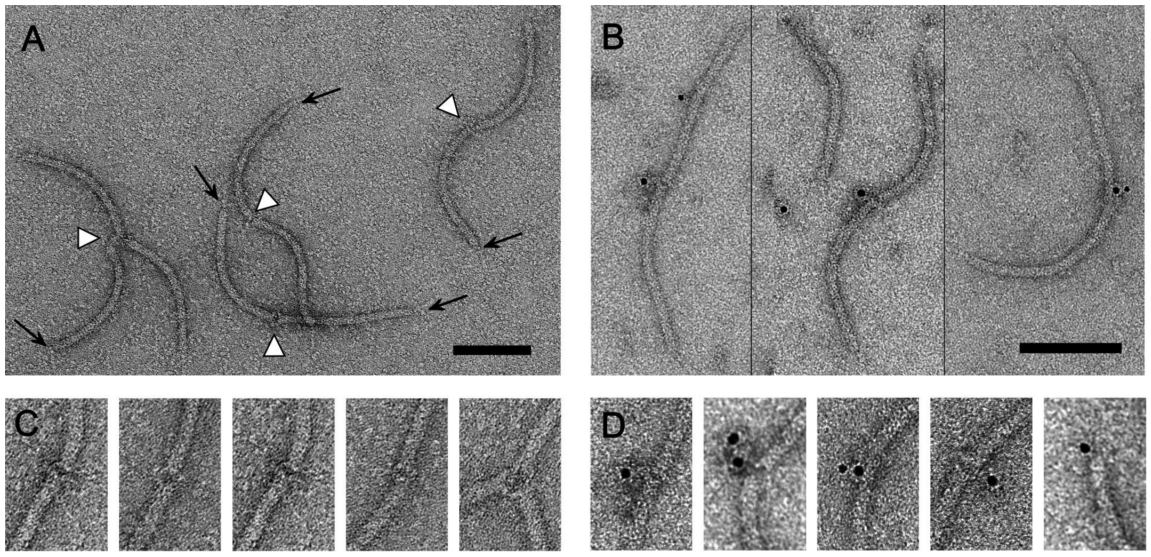

Fig. 4. Gp17 localization in the tail structure. Tails were incubated with purified IgG directed against gp17, negatively stained and observed by EM. The position of the antigen was identified by IgG cross-linking (white arrowheads in A) in A and C or visualization of the IgG molecule with anti-rabbit IgG complexed to colloidal gold in B and D. C and D show blow-up of the immunolabelled tail end distal from the tail spike (black arrows in A). The scale bars represent 100 nm.

IgG cross-linking (Fig. 4A and C) or visualization of the IgG molecule with anti-rabbit IgG complexed to colloidal gold (Fig. 4B and D). Gp17 is localized at the top of the tail end opposite to the tail spike. No labelling was observed in intact phage particles strongly suggesting that gp17 is buried in the tail-to-head interface and therefore inaccessible for IgG labelling in SPP1 virions (data not shown).

Gp17 is a monomer in solution

The gp17 thin ring observed by EM suggests that the functional state of the protein corresponds to an oligomer. Its structure thus needs to accommodate a central channel large enough to allow the passage of DNA during infection. Based on phage lambda gpU structural data (Pell *et al.*, 2009) and on the gp17 model proposed by Chagot *et al.* (2012) this oligomer probably corresponds to a hexamer.

Recombinant gp17 overproduced in *Escherichia coli* was mainly recovered in the soluble fraction of crude lysates and purified in a single step of metal affinity chromatography (Fig. 5A; Chagot *et al.*, 2012). 6His-gp17 or gp17-6His proteins were eluted at a concentration of 250 mM imidazole from a Ni-NTA column. The protein was highly pure as judged from the single band on a 16% SDS-polyacrylamide gel (Fig. 5A). The method yielded about 5 to 10 mg of pure protein from 1 l of culture. After cleavage of the tag with Tobacco Etch Virus (TEV) protease, gp17 eluted as a single peak from size exclusion chromatography in a Superdex 200 column (Fig. 5B, solid curve). The elution K_{av} (≈ 0.65) was the one expected for a protein with an apparent molecular mass of 14.5 kDa compatible with the theoretical mass (15.3 kDa) of a globular monomer of gp17.

Experiments with the gp17 structurally related protein gpU of phage lambda showed that addition of 20 mM of Mg^{2+} led to the association of gpU monomers to ring-shaped hexamers (Katsura and Tsugita, 1977; Edmonds *et al.*, 2007). This property was explained by the neutralization of clusters of acidic residues on the GpU surface that can bind Mg^{2+} rather than by a physiological role of the cation (Edmonds *et al.*, 2007). In contrast, gp17 was strictly monomeric in all buffer conditions assayed including the addition of high concentrations of magnesium (up to 100 mM) (Fig. 5B, dotted curve). Structural alignment of gpU and gp17 shows that the patch of acidic residues found in gpU that are necessary for the magnesium-dependent oligomerization are absent in gp17 providing a plausible explanation for the different behaviour of the two proteins in presence of the divalent cation.

Assembly in vivo *of SPP1 particles with engineered gp17 versions*

The biological activity of the amino and carboxyl-terminus tagged gp17 proteins in phage assembly was assessed by complementation in plate titration assays. SPP1*sus82* was complemented (> 90%) in the non-permissive *B. subtilis* strain YB886 bearing pIA21 or pIA22 that encode 6His-gp17 and gp17-6His respectively. Viral particles assembled under *in vivo* complementation conditions with

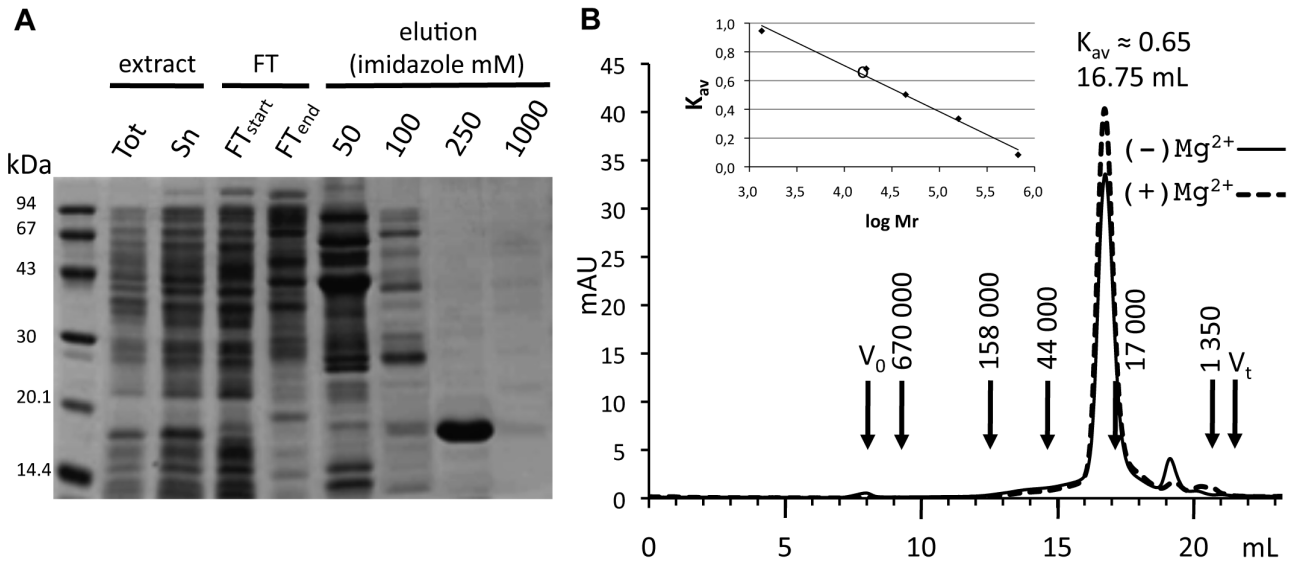

Fig. 5. Gp17 purification and size exclusion chromatography analysis.
A. Coomassie Blue-stained SDS-PAGE gel (16% polyacrylamide) showing the gp17 purification steps by Ni-NTA affinity chromatography. The migration of molecular mass markers is shown on the left. Tot: total extract; Sn: soluble fraction; FT: flow-through.
B. Analytical size exclusion chromatography of gp17. Purified gp17 incubated at 4°C for 16 h in the presence (dotted curve) or absence (solid curve) of 100 mM $MgCl_2$ (60 µl sample at 3.5 mg ml^{-1}) was applied to a 24 ml Superdex 200 column. The run was performed with a flow rate of 1 ml min^{-1} at 4°C with continuous monitoring of the eluting material at an absorbance of 280 nm. The column void volume (V_0) determined with blue dextran 2000, the column total volume (V_t) determined with acetone, and the volume of elution (V_e) of standard proteins with the mass shown (thyroglobulin, 670 kDa; gammaglobulin, 158 kDa; ovalbumin, 44 kDa; myoglobin, 17 kDa; and vitamin B12, 1.35 kDa) are indicated by vertical arrows. Inset, plot of K_{av} $[(V_e - V_0)/(V_t - V_0)]$ versus log molecular weight for protein standards. Gp17 (open circle) estimated to have a molecular weight of ~ 14 500 Da.

gp17-6His yielded one single band after isopycnic centrifugation in CsCl gradients (Fig. 6A), corresponding to infective phage particles (EM observations not shown). Complementation with 6His-gp17 led to presence of the phage particles band but also of a second well-resolved band containing denser tailless capsids filled with DNA (Fig. 6A; data not shown). The latter structures are predominant in the control experiment when no plasmid-encoded gp17 was produced in bacteria infected by SPP1*sus82*. The hexahistidine-tag at the gp17 amino-terminus position thus reduces the efficiency of the tail-to-head joining reaction resulting in accumulation of DNA-filled capsids non-associated to tails. In contrast, gp17-6His provided *in trans* allowed to join together all tails and DNA-filled capsids produced in the infected cells. The progeny phages were genotypically SPP1*sus82*, infecting the suppressor strain *B. subtilis* HA101B but not the non-suppressive host *B. subtilis* YB886.

The electrophoretic behaviour of 6His-gp17 and gp17-6His proteins produced in *E. coli* and *B. subtilis* was identical (Fig. 6B, compare lanes 3 and 4 with 5 and 6). However, 6His-gp17 incorporated in viral particles resulting from complementation experiments had an intermediate electrophoretic mobility between free hexahistidine-tagged protein and non-tagged gp17 (lane 8 in Fig. 6B). This result indicates that the phage particle assembly reaction leads to the selective incorporation of a gp17 form that lost part of the 15-amino-acid-long tag at the gp17 amino-terminus position which might result from proteolysis of the engineered tag during assembly. It provides also an explanation for the less efficient formation of complete phage particles when SPP1*sus82* is complemented by 6His-gp17 in non-permissive infections (Fig. 6A; see above).

Reconstitution of the tail-to-head joining reaction in vitro

We have developed an *in vitro* complementation assay adapted from Dröge and Tavares (2000) to study the incorporation of gp17 or of purified tails during assembly of infectious particles in extracts of infected cells. Donor extracts were prepared from lysates of non-permissive bacteria infected with SPP1 mutants blocked either in tail tube assembly (SPP1*sus45*) or in tail-to-head joining (SPP1*sus82*). Non-permissive infection with mutant SPP1*sus45,* which is impaired in gp17.1 and gp17.1* production (Auzat *et al.*, 2008), leads to the accumulation of DNA-filled capsids and gp17. SPP1*sus82*-infected cells were the source of both DNA-filled capsids and tails without gp17. We added SPP1*sus31* purified tails, SPP1*sus82* purified tails, gp17, or water to the extracts and scored for assembly of infectious particles. Phage titration

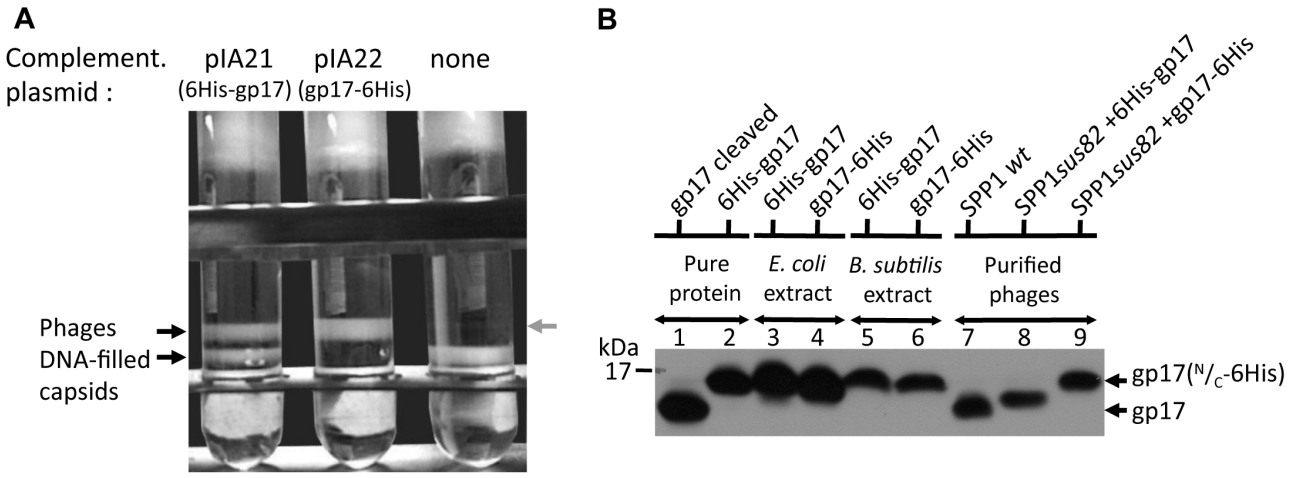

Fig. 6. Assembly of SPP1 virions with tagged gp17.
A. Isopycnic centrifugation of phages produced during SPP1*sus82* infection of YB886 bearing plasmids pIA21 coding for 6His-gp17, pIA22 coding for gp17-6His, or no plasmid (control). The picture shows tubes after centrifugation of the virions through a discontinuous density gradient with preformed layers of 1.7, 1.5 and 1.45 g cm^{-3} CsCl in TBT buffer. The upper band corresponds to entire phage particles and the lower band to tailless capsids filled with DNA as assessed by EM (not shown). The grey arrow highlights a weak phage band.
B. Tagged gp17 forms in bacterial extracts and purified SPP1 particles. Proteins were separated in a 16% SDS-PAGE and gp17 was detected by Western blot with a rabbit polyclonal antiserum. Samples are 6His-gp17 after cleavage with TEV (lane 1) and uncleaved (lane 2), crude extracts from *E. coli* BL21 DE3 overnight cultures bearing pIA21 (lane 3) or pIA22 (lane 4), crude extracts from *B. subtilis* YB886 overnight cultures bearing pIA21 (lane 5) or pIA22 (lane 6), and proteins of CsCl purified phage particles [lane 7: phages produced by infection of YB886 with SPP1 wild type; lane 8: phages produced by infection of YB886 (pIA21) with SPP1*sus82*; lane 9: phages produced by infection of YB886 (pIA22)].

was carried out in the permissive strain HA101B because the viral particles assembled *in vitro* were genotypically *sus* mutants. The maximal yield of phage production was approximately 10^{10} pfu ml^{-1} in the assembly reaction. A background of about 10^5–10^6 pfu ml^{-1} is attributed to infection by revertants in the SPP1*sus* lysates (assay 1 in Fig. 7). Note that a very thin phage band was also present in the CsCl gradient in *sus82* infections under non-complementing conditions (grey arrow in Fig. 6A). As expected, complete SPP1*sus31* purified tails were able to complement both SPP1*sus82* and SPP1*sus45* extracts by joining directly to DNA-filled capsids for assembly of infective virions (assay 2 in Fig. 7). When we mixed SPP1*sus82* purified tails, devoid of gp17, with SPP1*sus45* extracts, assembly of infectious particles was observed showing that endogenous gp17 in the extract was able to be incorporated at the tail end distal from the tail spike which subsequently binds to capsids producing virions (blue in assay 3 of Fig. 7). This reaction reached a yield identical to the one found for the simple tail-to-head joining reaction with wild-type tails (assay 2). The assembly reaction was remarkably reproducible and purified tails were stable over time yielding similar results after storage for several weeks at 4°C. Tails purified from SPP1*sus82* infections did not complement *sus82* cellular extracts, as expected (red in assay 3 of Fig. 7). A fivefold increase above the background titre is attributed to the presence of a minor population of wild-type tails in the SPP1*sus82* tails preparation.

Last but not least, the addition of monomeric purified gp17, with or without hexahistidine-tag, to SPP1*sus82* extracts was necessary and sufficient to stick together capsids and tails with an efficiency identical to the one found for complementation with purified tails (red in assay 4 of Fig. 7).

Discussion

Bacteriophage SPP1 gp17 is encoded by gene *17* which is localized between the head and tail morphogenesis operons (Fig. 1B). Its absence during infection leads to assembly of DNA-filled heads and tails that do not stick together (Fig. 2A), showing that gp17 is essential for the tail-to-head joining reaction. Tails with normal morphology, length and sedimentation behaviour are assembled in its absence (Figs 2 and 3), but lack biological activity in an *in vitro* phage assembly assay in crude extracts which was developed in this work (Fig. 7). Detailed inspection of electron micrographs showed that the end of these tails distal from the tail tip is characterized by a sharp cut of the tail tube (Fig. 2I) and in some cases a fuzzy or corolla-like appearance is observed (rectangle in Fig. 2E) which we attribute to locally confined disassembly of the tube. In contrast, tails competent for virus assembly are tapered by a thin ring narrower than the tube diameter (Fig. 2J) which we identify as gp17. Immuno-EM confirmed this assignment (Fig. 4). Addition of purified gp17 was sufficient to render gp17-deficient tails competent to assemble into

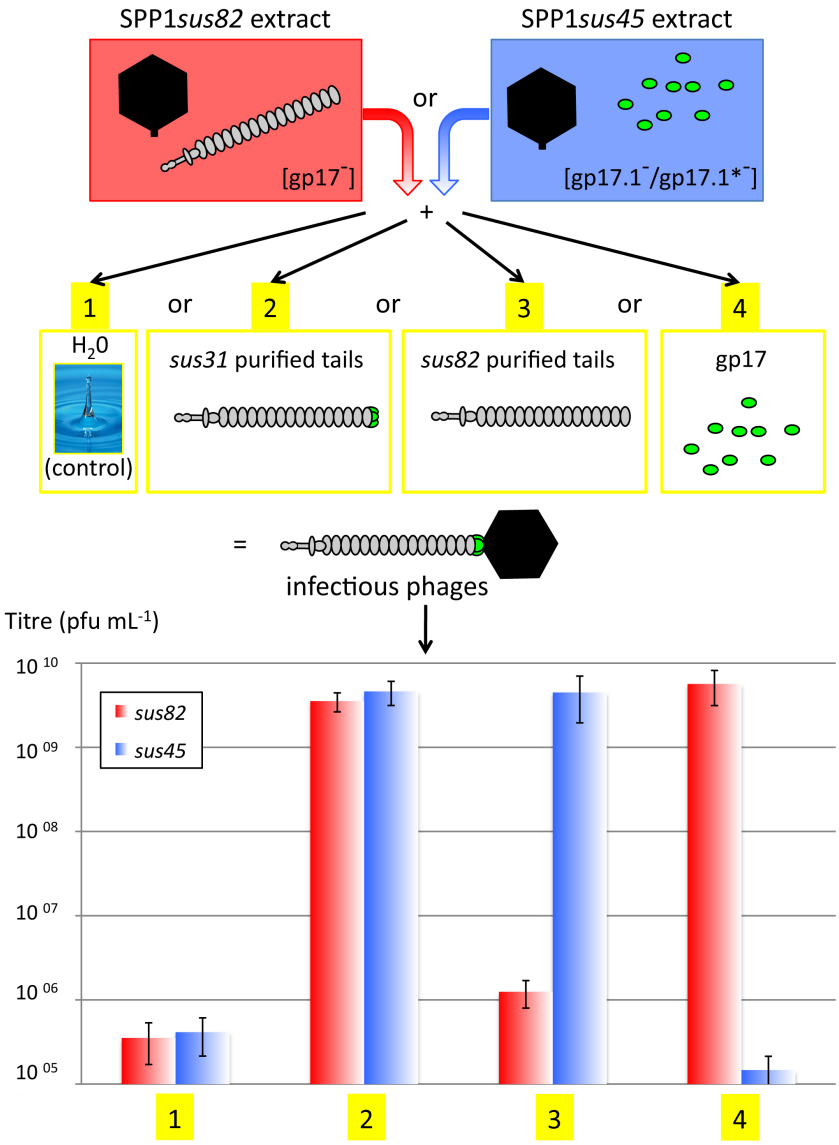

Fig. 7. *In vitro* assembly assay. The upper part of the figure shows a schematic representation of the phage structures and gp17 (green ovals) found in the two donor extracts used. Extracts from *B. subtilis* YB886 infected with the tail-to-head joining protein (gp17⁻)-deficient mutant SPP1*sus82* or with the tail tube proteins (gp17.1⁻/gp17.1*⁻)-deficient mutant SPP1*sus45* are represented in red and blue respectively. Each extract was mixed separately with four different purified components identified by yellow rectangles (1: water, control; 2: complete tails purified from SPP1*sus31* extracts, i.e. having gp17; 3: tails devoid of gp17 purified from SPP1*sus82* extracts; 4: purified gp17). After incubation, the progeny was determined by titration of the final supernatant on the permissive host *B. subtilis* HA101B. The bottom graph shows the titres obtained for SPP1*sus82* or SPP1*sus45* extracts in red and blue, respectively, mixed with the components 1, 2, 3 or 4 described above. Error bars represent the standard deviation from five independent experiments.

infectious virions *in vitro* (Fig. 7). The assay thus reconstitutes the reactions of gp17 binding to the tail end and subsequent attachment to DNA-filled capsids that terminate SPP1 morphogenesis. Joining of the tail to the head shields gp17 from immunolabelling indicating that its narrow ring becomes at least partially buried in the tail-to-head interface of infectious virions. The data presented here show that gp17 acts at a late stage of SPP1 assembly binding to the helical tail tube end and that its function is to provide an interface for tail attachment to DNA-filled capsids. We thus designate it as the tail-to-head joining protein (THJP).

Purified gp17 overproduced in the heterologous host *E. coli* is active in SPP1 assembly reactions *in vitro*. The protein is a monomer at millimolar concentrations in all buffer conditions tested (Chagot *et al.*, 2012; Fig. 5; data not shown). Assembly of a ring at the tail end results conceivably from gp17 multimerization probably forming a hollow hexamer as proposed for the structurally related protein gpU of phage lambda (Pell *et al.*, 2009; Chagot *et al.*, 2012). This organization matches the sixfold symmetry of the SPP1 helical tail (Plisson *et al.*, 2007) and can also adapt to the 12-fold symmetry of gp16 which forms the connector interface for tail attachment in DNA-filled capsids (Lhuillier *et al.*, 2009). The quaternary structure of gp17 is thus only acquired when it contacts its previously assembled partner, the tail tube, leading to a conformation suitable to participate in the subsequent tail-to-head stable binding reaction. Non-assembled gp17 and gpU, like numerous phage structural proteins, are characterized by the presence of disordered and flexible regions (Edmonds *et al.*, 2007; Chagot *et al.*, 2012). Their folding promoted by

interaction with an assembly intermediate is a recurrent strategy to build new contact surfaces competent for protein–protein interaction. This selective mechanism ensures the sequential assembly of supramacromolecular structures composed of many copies of several different proteins like phage tails and connectors (Lhuillier *et al*., 2009; Pell *et al*., 2009; Davidson *et al*., 2012; Tavares *et al*., 2012).

Lambda gpU, like gp17, binds to the tail tube only once it reaches the correct length that is determined by the TMP gpH as elegantly shown by Katsura (1987). TMPs are ubiquitous length rulers in *Sipho-* and *Myoviridae* tails. They likely expand through the entire length of the tail tube. In SPP1 tails, they correspond to a continuous internal density in EM reconstructions discernible before DNA ejection but absent after DNA release through the tube (Plisson *et al*., 2007). The TTP gpV of phage lambda assembles elongated structures called polytubes that can grow to a length of several microns, in absence of TMP, if a complex of the tail tip proteins gpM and gpL is present to act as an initiator for gpV polymerization (Katsura and Kühl, 1974). Growth of polytubes can be stopped by the addition of gpU *in vitro* (Katsura and Tsugita, 1977), independently of their length, consistent with its capacity to bind polymers of gpV and block concomitantly their elongation. Polytails carrying gpU bind DNA-filled capsids showing that gpU renders tail tubes competent for association to phage heads (Katsura and Kühl, 1975a). In the normal tail building pathway, polymerization of gpV marks a pause at the correct tail length leading to the formation of gpU$^-$ tails (Katsura, 1976). If gpU does not bind during the pause of gpV assembly, polymerization resumes yielding a dominant population of polytails (Pell *et al*., 2009) which have lost gpH (Katsura, 1976) and do not interact with capsids. In presence of gpU, approximately 10 kDa of the TMP gpH are cleaved off from its carboxyl-terminus originating gpH* (Walker *et al*., 1982). This cleavage occurs after the stop of gpV polymerization and gpU binding (Tsui and Hendrix, 1983). The resulting tails bind to lambda capsids building correctly shaped phage particles but those particles show much reduced infectivity (Casjens and Hendrix, 1974) unless assembly of the tail-to-head interface occurred in presence of gpZ. Neither the location of gpZ within phage particles nor its mechanism of action are known (Davidson *et al*., 2012). Assembly of a predominant population of long polytails in the absence of a gpU-like protein is at present a rather unique feature of phage lambda. Mutants of phages P2 (gpR; Lengyel *et al*., 1974), SPO1 (gp8; Parker and Eiserling, 1983), Mu (gpK; Grundy and Howe, 1985) and T4 (gp3; Vianelli *et al*., 2000) lacking their putative THJP mainly build tails of a normal size but feature also longer tails whose size does not exceed three times the usual tail length in most cases. Assembly of the long non-contractile tube of bacteriophage SPP1 tail is achieved by polymerization of the TTPs gp17.1/gp17.1* leading to a helical array of TTP hexamers organized around the TMP gp18 (Plisson *et al*., 2007) as described for lambda. In contrast, termination of tail tube elongation is achieved in absence of the THJP showing that this protein is not required to control length of the SPP1 tail being only necessary for tail binding to capsids (this work).

A model for tail length determination in wild type and in THJP$^-$ mutants of phages SPP1 and lambda is shown in Fig. 8. Present knowledge is consistent with a mechanism in which an interaction between the protuberant extremity of the TMP and the last growing ring of the TTP in the tail tube stops tube elongation ensuring formation of tails whose size is proportional to the tape measure length (Katsura and Hendrix, 1984). The stability of this association is proposed to differ among phages explaining the distinct phenotypes found in absence of THJP proteins as typified by SPP1 and lambda. A strong interaction would freeze the complex, yielding a population of normally sized tails as in case of SPP1 where the last TTP ring remains inactive (black oval in Fig. 8) to promote further polymerization of TTP subunits. A weaker interaction permits the tube top TTP ring to switch after a pause from an inactive (black oval in Fig. 8) to a polymerization-competent state (grey oval) if the THJP does not taper the tail tube. The strength of the TMP extremity-TTP interaction would control the frequency of this switch and thus of resumption of tail tube polymerization accounting for the variable THJP$^-$ phenotypes found for phages P2, SPO1, Mu, T4 and lambda. In the case of lambda, it was reported that polytails lack the TMP, the release of which could in fact support polytail formation by providing a scaffold for TTP polymerization as it exits the tube (Fig. 8, bottom panel). Our work shows that the conserved function of THJP proteins, previously called Tail Terminator Proteins (TrP; Davidson *et al*., 2012), is to build a ring at the top of the tail tube that provides the interface for binding to the connector of DNA-filled capsids rather than tail polymerization termination as normally described. The THJP interaction with the tube end tapers the structure supporting in some phages the definite arrest of TTP polymerization which is primarily determined by the TMP after the tube reaches its correct size.

Experimental procedures

Materials

Molecular biology reagents were from Invitrogen (Carlsbad, USA), New England Biolabs (Ipswich, USA), Roche Applied Science (Mannheim, Germany) and Stratagene (La Jolla, USA). Oligonucleotides were synthesized at MWG Biotech AG (Ebersberg, Germany).

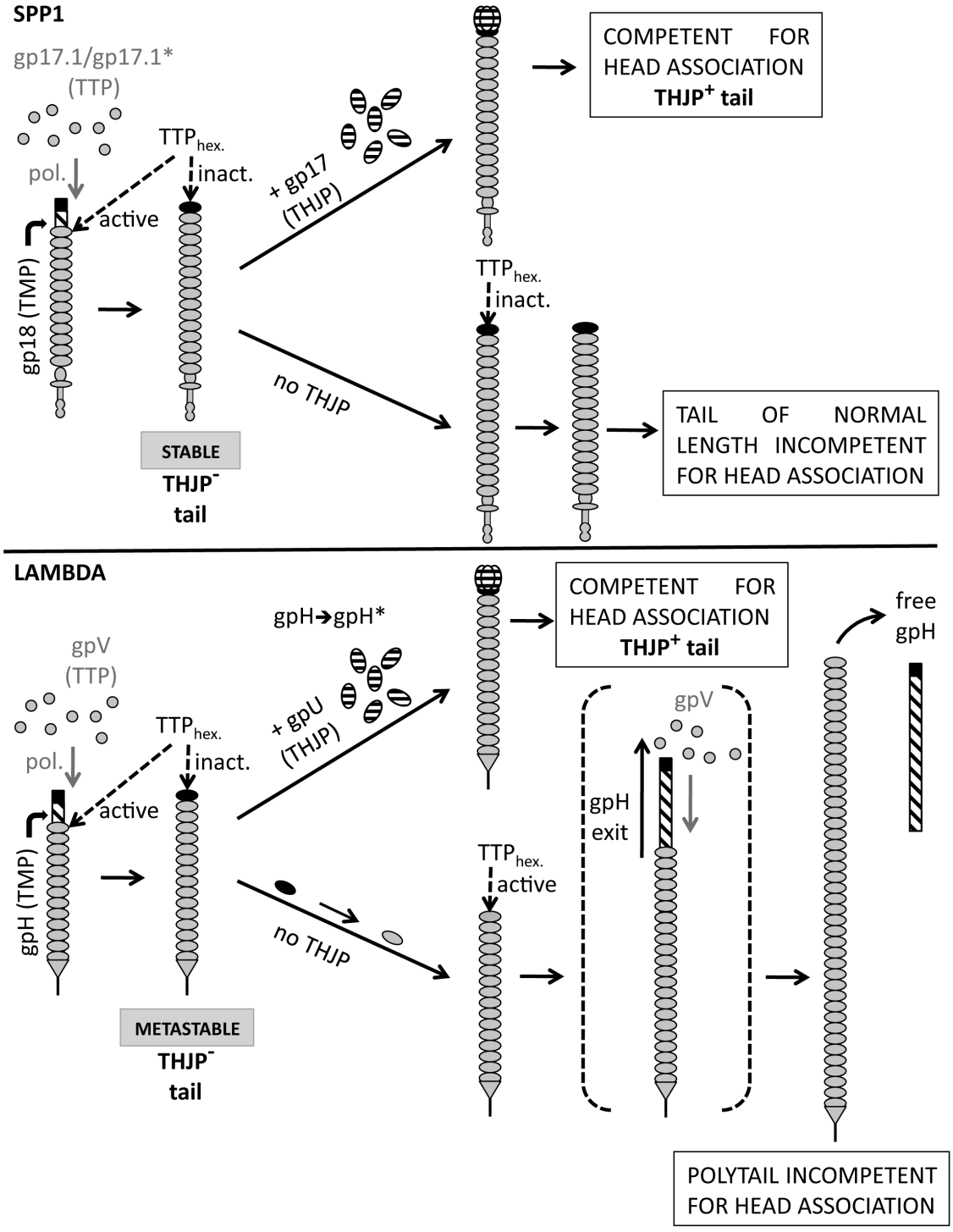

Fig. 8. Comparison of the last stages of tail assembly of bacteriophages SPP1 (upper part) and lambda (lower part) and model for tail control length. Gp17⁻ and gpU⁻ infections lead to the production of correctly sized tails (SPP1; this work) and to a predominant population of tails of variable length significantly longer than normal tails (lambda polytails; Katsura, 1976; Pell *et al.*, 2009) respectively. Gp17 and gpU are represented as black and white dashed ovals. The tail spike and TTP (circles in the non-assembled form and ovals in the assembled tail tube) are rendered in light grey while the TMP is shown as a diagonally dashed rectangle whose extremity protruding from the tail tube is in black. Dotted arrows highlight the conformational state of the last ring of the tail tube TTP with a grey oval representing a hexamer active for TTP polymerization and the black oval an inactive conformation. Activity of the tail structures for assembly into infective virions is displayed inside rectangles. gpH* is the carboxyl-terminus cleaved form of gpH whose processing depends on the presence of gpU (Tsui and Hendrix, 1983).

Table 1. Oligonucleotides used in this work.

Name	Sequence	Restriction sites
60331AZ	GG*GAATTC*aaaggagAA*GGATCC***ATG**ACATGGAAACTAGCC	EcoRI, BamHI
60603AZ	CC*GGTACCCTGCAG*GGCTGAACCCGTTGCC	KpnI, PstI
1F-SrbsNhisTEV	*GTCGAC*aaaggagAAATT*CAT**ATG*** CATCACCATCACCATCACGAGAATCTGTATTTCCAAGG	SalI, NdeI
2F-TEVPx	GAGAATCTGTATTTCCAAGGC *CTGCAG*atgccacaactgcctggg	PstI
3F-SrbsNPx	*GTCGAC*aaaggagAAATT*CAT**ATG**CTGCAG*atgccacaactgcctggg	SalI, NdeI, PstI
4R-xATEV	TGATGGCCTTGGAAATACAGATTCTC *ACCGGT*tgaccctctcgccaacct	AgeI
5R-TEVhisStopBHS	*GTCGACAAGCTTGGATCC***TCA** GTGATGGTGATGGTGATGGCCTTGGAAAT	SalI, HindIII, BamHI
6R-xAStopBHS	*GTCGACAAGCTTGGATCC***TCA***ACCGGT*tgaccctctcgccaacct	SalI, HindIII, BamHI, AgeI
F-gp17	**ATG***CTGCAG*ACATGGAAACTAGCCTCA	PstI
R-gp17	**TCA***ACCGGT*ATTGTTGTTTATGGTGAA	AgeI

The sequence complementary to the 3′ terminus region of *B. subtilis* 16S RNA (Moran *et al*., 1982) are in lowercase and underlined and the translation signals are in bold. Sequences homologous to SPP1 are in uppercase and underlined while irrelevant gene coding sequences are in lowercase. Relevant restriction sites are in italics. Sequence coding for histidine residues are in white boxes and partial or complete sequence coding ENLYFQG featuring a recognition site for TEV protease are in grey boxes.

Escherichia coli DH5α was used for all cloning procedures while *E. coli* JS218 (Bergès *et al*., 1996) or BL21 (DE3) strains were used for overproduction of gp17. *B. subtilis* YB886 (Yasbin *et al*., 1980) was used as non-permissive strain and to bear plasmids coding for different gp17 forms in *in vivo* and *in vitro* complementation assays. *B. subtilis* HA101B (*sup-3*; Okubo and Yanagida, 1968) was the permissive host for bacteriophages SPP1*sus31* (Becker *et al*., 1997), SPP1*sus45* (Behrens *et al*., 1979; Auzat *et al*., 2008) and SPP1*sus82* (Behrens *et al*., 1979; this work).

Phage production, purification and genome sequencing

Phages SPP1*sus31*, SPP1*sus45* and SPP1*sus82* were amplified by infection of the *B. subtilis* HA101B permissive strain as described (Chai *et al*., 1992). Phage titre and reversion rates in the lysates were determined by titration in strains HA101B and YB886 respectively. The mutation *sus82* was mapped in gene *17* by marker rescue in *B. subtilis* YB886 (pBT367). Gene *17* was amplified by PCR using phage SPP1*sus82* purified DNA as template followed by its complete sequencing at the MPI-MG sequencing facility to identify the mutation. Production of phages carrying a hexahistidine tag in the amino or carboxyl-termini of gp17, was carried out by infection with SPP1*sus82* of *B. subtilis* YB886 bearing plasmids pIA21 or pIA22 respectively. Culture infection and phage purification through a discontinuous CsCl density gradient with preformed layers of 1.7, 1.5 and 1.45 g cm^{-3} CsCl were carried out as described (Sambrook *et al*., 1989; Auzat *et al*., 2008).

Plasmid construction

Gene *17* was amplified by PCR using primers 60331AZ and 60603AZ (Table 1). The PCR fragment cleaved with EcoRI–PstI was cloned into vector pBluescript pSK- (Stratagene) cleaved with the same enzymes generating pSK18. This fragment was then excised by restriction from pSK18 and ligated to pHP13 cut with EcoRI–PstI to yield pBT367.

The shuttle vector pHP13 which replicates both in *E. coli* and in *B. subtilis* cells under the control of the inducible promoter PN25/0 (Haima *et al*., 1987; Le Grice, 1990) was engineered to allow the cloning of cassettes into its SalI restriction site. First, one of the PstI sites present in the plasmid pHP13 polylinker was eliminated by cleavage with SwaI and NdeI flanking this PstI site. Blunt ends were generated by filling-in with T4 DNA polymerase in the presence of dNTPs and subsequent ligation. The resulting plasmid pIV2 was digested by PstI in order to delete the second PstI site. This cleavage was followed by fill-in of the 5′ overhangs and by a ligation step generating the vector pIA1. Cassette 1 adds a tail to the amino-terminus of the gene of interest featuring an initiation codon, a hexahistidine tag and a recognition sequence for cleavage by TEV protease. Cassette 2 adds a tail to the carboxyl-terminus of the gene coding for a stop codon, a recognition sequence for cleavage by TEV protease and a hexahistidine tag. Within each cassette, a 3′-PstI and 5′-AgeI restriction sites are present allowing the cloning of any gene of interest. We used a two-step PCR amplification procedure to create the cassettes with a plasmid coding for an irrelevant 600 bp gene insert as template. Cassette 1 was successively amplified with primers 2F-TEVPx + 6R-xAStopBHS and 1F-SrbsNhisTEV + 6R-xAStopBHS (Table 1). Cassette 2 was amplified with primers 3F-SrbsNPx + 4R-xATEV and 3F-SrbsNPx + 5R-TEVhisStopBHS (Table 1). In both cases, 10 μl of the first PCR mixture was used as a template for the second PCR with an excess of four times of the second primer set, in a total volume of 50 μl. Each purified cassette cleaved with SalI was cloned into plasmid pIA1 digested with the same restriction enzyme generating the shuttle vectors pIA2 (amino-terminus hexahistidine tag) and pIA3 (carboxyl-terminus hexahistidine tag) respectively.

A 399 bp fragment covering the gene *17* sequence (position from 10 066 to 10 464 of the SPP1 nucleotide sequence; access code X97918.2) lacking the initiation and stop codons was amplified by PCR from SPP1*wt* DNA with two flanking sequences coding for a 3′-PstI and 5′-AgeI restriction sites. Oligonucleotides F-gp17 and R-gp17 (Table 1) were used as forward and reverse primer respectively. The purified PCR

product was totally sequenced at GATC Biotech (Konstanz, Germany), subsequently cleaved with PstI and AgeI and inserted into the pIA2 and pIA3 shuttle vectors digested by the same restriction enzymes. The resulting plasmids were named pIA21 (6His-gp17) and pIA22 (gp17-6His).

Protein production, purification and antibodies production

Escherichia coli JS218 strain freshly transformed with plasmids pIA21 or pIA22 was grown at 37°C in Luria–Bertani broth supplemented with erythromycin (30 μg ml^{-1}) and chloramphenicol (10 μg ml^{-1}) until reaching an absorbance at 600 nm of 0.5–0.6. Then, cultures were induced with 2 mM IPTG for 2 h. Pelleted bacteria were resuspended and disrupted by sonication. Crude extracts were centrifuged at 4°C twice for 20 min at 27 000 *g*. Imidazole was then added to a final concentration of 20 mM and recombinant hexahistidine-tagged gp17 proteins were purified by metal-chelating chromatography using a 5 ml Hi-Trap Ni-NTA column (GE Healthcare) pre-equilibrated with buffer A (20 mM NaH_2PO_4, pH 7.4, 500 mM NaCl). The column was washed with increasing concentrations of buffer B (buffer A containing 1 M imidazole), eluted at 250 mM imidazole and the eluate was concentrated by ultrafiltration (Vivaspin 20, 5 kDa molecular mass cut-off). At this step, the protein was more than 95% pure as assessed by Coomassie Blue staining of SDS-PAGE (Fig. 5A). Removal of the hexahistidine tag from gp17 was performed by incubation of the protein at 1 mg ml^{-1} with His6-TEV protease at a ratio of 1:20 (w/w) in the elution buffer (buffer A containing 250 mM imidazole) supplemented with 1 mM DTT and 5 mM EDTA at 4°C for 16 h. The samples were diluted in buffer A to decrease imidazole concentration to 75 mM and run through the same 5 ml Ni-NTA-column pre-equilibrated with buffer A in order to remove the tag, uncleaved protein and protease.

The gp17 concentration was determined according to Bradford (1976) using immunoglobulins as a standard or by measurement of the UV absorbance at 280 nm, with a theoretical extinction coefficient of 16 960 M^{-1} cm^{-1}.

Rabbit polyclonal antibodies raised against purified and cleaved gp17 were produced at the INAF platform (CNRS, Gif-sur-Yvette).

Determination of the oligomeric state of gp17

Analytical size exclusion chromatography was carried out in a 24 ml Superdex 200 column (GE Healthcare) in buffer C (20 mM Tris-HCl, pH 8.5, 50 mM NaCl). The column was calibrated with one vial of protein standards mixture containing thyroglobulin (670 kDa), γ-globulin (158 kDa), ovalbumin (44 kDa), myoglobin (17 kDa) and vitamin B12 (1.35 kDa) (Bio-Rad) (Fig. 5B) resuspended in 500 μl of buffer C. The column void volume (V_0) and the total volume (V_t) were determined using the elution volumes of blue dextran 2000 and acetone respectively. Gp17 protein samples concentrated at 3.5 mg ml^{-1} were applied on the column after incubation at 4°C for 16 h in the presence or absence of 100 mM $MgCl_2$. The molecular mass of native gp17 was estimated by plotting the partition coefficient K_{av} against the log of relative molecular mass for the standards. $K_{av} = (V_e - V_0)/(V_t - V_0)$, where V_e is the elution volume of the protein under analysis.

Preparation and analysis of bacterial extracts

Extracts of *E. coli* and *B. subtilis* were prepared and analysed by Western blot as described (Auzat *et al.*, 2008; Isidro *et al.*, 2004 respectively).

*Tail purification from SPP1*sus31 *and SPP1*sus82 *mutants*

Tail structures were purified from lysates of *B. subtilis* YB886 infected with the SPP1*sus31* or SPP1*sus82* mutants using the method of A. Seul (unpublished) with a few modifications. Briefly, a 130 ml LB culture of the host strain, grown to OD_{600} = 0.8 and supplemented with 10 mM $CaCl_2$, was divided in two for parallel infections, at an input multiplicity of 5 phages/bacterium. After 1 h shaking at 37°C the completion of lysis, reduction of viscosity, and protein integrity in the extracts were achieved by an additional 10 min incubation in the presence of 200 μg ml^{-1} of lysozyme, 10 μg ml^{-1} DNase, 100 μg ml^{-1} RNase and Roche complete protease inhibitors as recommended by the manufacturer. Capsid and/or tail structures produced in the lysates were enriched by centrifugation through a 20% sucrose cushion in TBT buffer (100 mM Tris-HCl, pH 7.5, 10 mM $MgCl_2$, 100 mM NaCl) at 32 000 r.p.m., 4°C for 18 h in a SW41 rotor. Supernatants were removed leaving about 500 μl per tube to resuspend the pellets which were kept at 4°C overnight. The following day, the buffer was exchanged for sucrose-free TBT using Vivaspin 20 devices (10 kDa molecular mass cut-off) and concentrated pellets were sedimented through a 10% to 30% (w/v) glycerol gradient for 6 h in a SW41 rotor. The resulting fractions were analysed by SDS-PAGE and Western blot using anti-SPP1 serum. The most enriched fractions in tail structures were pooled and diluted in buffer without salt Q-A (100 mM Tris-HCl, pH 7.5, 10 mM $MgCl_2$) down to a final concentration of 50 mM NaCl and loaded onto a 6 ml anion exchange column (resource Q, GE Healthcare). Purification was performed with two consecutive gradients using buffer Q-B (100 mM Tris-HCl, pH 7.5, 10 mM $MgCl_2$, 2 M NaCl) of 0 M to 0.5 M NaCl (7 column volumes) and 0.5 M to 2 M NaCl (1.5 column volumes) at a flow rate of 4 ml min^{-1}. Tail fractions were identified by Coomassie Blue-stained SDS-PAGE and Western blot analysis using rabbit polyclonal antibodies raised against SPP1 proteins and kept at 4°C for several months.

*Preparation of SPP1*sus45 *and SPP1*sus82 *extracts from infected cells for* in vitro *assembly*

Infection of *B. subtilis* YB886 cultures with SPP1*sus* mutants was carried out as described by Dröge and Tavares (2000). Seven minutes after infection, a polyclonal antiserum raised against SPP1 particles was added (5 μl per 2 ml of culture) to inactivate phages that did not adsorb to bacteria. Cultures at 35 min post-infection were split into identical volumes, centrifuged and the resulting pellets were maintained at 4°C. Buffer D [final concentration: 7.5 mM HEPES-KOH, pH 7.5,

7.5 mM potassium glutamate, 9 mM spermidine, 1.8 mM ATP, 9 mM $MgCl_2$, 10% Dextran (w/v)] and purified tails or gp17 were added on top of the pellet to a total volume of 50 µl. Spontaneous lysis of infected bacteria yielded reproducible extracts that were incubated for 90 min at 30°C. Cell debris was removed from the samples by centrifugation (20 min, 12 000 *g*, 4°C) and infectious phage progeny was quantified by titration of the final supernatant on the permissive host *B. subtilis* HA101B.

Electron microscopy

Aliquots of tail purification intermediate steps were imaged after negative staining with uranyl acetate (Steven *et al*., 1988).

For immunoelectron microscopy, purified tail structures were incubated with purified IgG for 3 to 12 h at room temperature. The immunocomplexes were pelleted by centrifugation in an Airfuge to remove unbound IgG and resuspended in TBT buffer. Part of the sample was prepared for EM by negative staining. The remaining material was used for incubation with goat anti-rabbit 5 nm gold conjugate (BBI solutions). After sedimentation of the conjugate-tail complexes in an Airfuge to eliminate free conjugates, the samples were negatively stained and observed by EM.

Acknowledgements

We thank Matthieu Cisel for carrying out some biochemical assays. Anait Seul is acknowledged for sharing the SPP1 tails purification method prior to publication. We thank Ines Vinga for her kind gift of pIV2 plasmid.

Research was supported by project Program Blanc from ANR (project 'DNA Gating') and by CNRS and MPG institutional funding.

References

Abuladze, N.K., Gingery, M., Tsai, J., and Eiserling, F.A. (1994) Tail length determination in bacteriophage T4. *Virology* **199:** 301–310.

Ackermann, H.W. (2007) 5500 Phages examined in the electron microscope. *Arch Virol* **152:** 227–243.

Aksyuk, A.A., and Rossmann, M.G. (2011) Bacteriophage assembly. *Viruses* **3:** 172–203.

Atia-tul-Wahab, Serrano, P., Geralt, M., and Wüthrich, K. (2011) NMR structure of the *Bordetella bronchiseptica* protein NP_888769.1 establishes a new phage-related protein family PF13554. *Protein Sci* **20:** 1137–1144.

Auzat, I., Dröge, A., Weise, F., Lurz, R., and Tavares, P. (2008) Origin and function of the two major tail proteins of bacteriophage SPP1. *Mol Microbiol* **70:** 557–569.

Becker, B., de la Fuente, N., Gassel, M., Günther, D., Tavares, P., Lurz, R., *et al*. (1997) Head morphogenesis genes of the *Bacillus subtilis* bacteriophage SPP1. *J Mol Biol* **268:** 822–839.

Behrens, B., Lüder, G., Behncke, M., Trautner, T.A., and Ganesan, A.T. (1979) The genome of *B. subtilis* phage SPP1: physical arrangement in phage genes. *Mol Gen Genet* **175:** 351–357.

Bergès, H., Joseph-Liauzun, E., and Fayet, O. (1996) Combined effects of the signal sequence and the major chaperone proteins on the export of human cytokines in *Escherichia coli*. *Appl Environ Microbiol* **62:** 55–60.

Bradford, M. (1976) A rapid and sensitive method for the quantitation of microgram quantities of protein utilizing the principle of protein-dye binding. *Anal Biochem* **72:** 248–254.

Casjens, S., and Hendrix, R. (1974) Comments on the arrangement of the morphogenetic genes of bacteriophage lambda. *J Mol Biol* **90:** 20–25.

Casjens, S., and Hendrix, R. (1988) Control mechanisms in dsDNA bacteriophage assembly. In *The Bacteriophages*, Vol. 1. Calendar, R. (ed.). New York: Plenum Press, pp. 15–91.

Chagot, B., Auzat, I., Gallopin, M., Petitpas, I., Gilquin, B., Tavares, P., and Zinn-Justin, S. (2012) Solution structure of gp17 from the Siphoviridae bacteriophage SPP1: insights into its role in virion assembly. *Proteins* **80:** 319–326.

Chai, S., Bravo, A., Lüder, G., Nedlin, A., Trautner, T.A., and Alonso, J.C. (1992) Molecular analysis of the *B. subtilis* bacteriophage SPP1 region encompassing genes *1–6*. The products of gene *1* and gene *2* are required for *pac* cleavage. *J Mol Biol* **224:** 87–102.

Davidson, A.R., Cardarelli, L., Pell, L.G., Radford, D.R., and Maxwell, K.L. (2012) Long noncontractile tail machines of bacteriophages. *Adv Exp Med Biol* **726:** 115–142.

Dröge, A., and Tavares, P. (2000) *In vitro* packaging of DNA of the *Bacillus subtilis* bacteriophage SPP1. *J Mol Biol* **296:** 103–115.

Edmonds, L., Liu, A., Kwan, J.J., Avanessy, A., Caracoglia, M., Yang, I., *et al*. (2007) The NMR structure of the gpU tail-terminator protein from bacteriophage lambda: identification of sites contributing to Mg(II)-mediated oligomerization and biological function. *J Mol Biol* **365:** 175–186.

Fokine, A., Zhang, Z., Kanamaru, S., Bowman, V.D., Aksyuk, A.A., Arisaka, F., *et al*. (2013) The molecular architecture of the bacteriophage T4 neck. *J Mol Biol* **425:** 1731–1744.

Goulet, A., Lai-Kee-Him, J., Veesler, D., Auzat, I., Robin, G., Shepherd, D.A., *et al*. (2011) The opening of the SPP1 bacteriophage tail, a prevalent mechanism in gram-positive-infecting Siphophages. *J Biol Chem* **286:** 25397–25405.

Grundy, F.J., and Howe, M.M. (1985) Morphogenetic structures present in lysates of amber mutants of bacteriophage Mu. *Virology* **143:** 485–504.

Haima, P., Bron, S., and Venema, G. (1987) The effect of restriction on shotgun cloning and plasmid stability in *Bacillus subtilis* Marburg. *Mol Gen Genet* **209:** 335–342.

Isidro, A., Santos, M.A., Henriques, A.O., and Tavares, P. (2004) The high-resolution functional map of bacteriophage SPP1 portal protein. *Mol Microbiol* **51:** 949–962.

Katsura, I. (1976) Morphogenesis of bacteriophage lambda tail. Polymorphism in the assembly of the major tail protein. *J Mol Biol* **107:** 307–326.

Katsura, I. (1987) Determination of bacteriophage lambda tail length by a protein ruler. *Nature* **327:** 73–75.

Katsura, I., and Hendrix, R.W. (1984) Length determination in bacteriophage lambda tails. *Cell* **39:** 691–698.

Katsura, I., and Kühl, P.W. (1974) A regulator protein for the length determination of bacteriophage lambda tail. *J Supramol Struct* **2:** 239–253.

Katsura, I., and Kühl, P.W. (1975a) Morphogenesis of the tail of bacteriophage λ. II. *In vitro* formation and properties of phage particles with extra long tails. *Virology* **63:** 238–251.

Katsura, I., and Kühl, P.W. (1975b) Morphogenesis of the tail of bacteriophage lambda. III. Morphogenetic pathway. *J Mol Biol* **91:** 257–273.

Katsura, I., and Tsugita, A. (1977) Purification and characterization of the major protein and the terminator protein of the bacteriophage lambda tail. *Virology* **76:** 129–145.

Le Grice, S.F.J. (1990) Regulated promoter for high-level expression of heterologous genes in *Bacillus subtilis*. *Methods Enzymol* **185:** 201–214.

Lengyel, J.A., Goldstein, R.N., Marsh, M., and Calendar, R. (1974) Structure of the bacteriophage P2 tail. *Virology* **62:** 161–174.

Lhuillier, S., Gallopin, M., Gilquin, B., Brasilès, S., Lancelot, N., Letellier, G., *et al*. (2009) Structure of bacteriophage SPP1 head-to-tail connection reveals mechanism for viral DNA gating. *Proc Natl Acad Sci USA* **106:** 8507–8512.

Moran, C.P., Jr, Lang, N., LeGrice, S.F., Lee, G., Stephens, M., Sonenshein, A.L., *et al*. (1982) Nucleotide sequences that signal the initiation of transcription and translation in *Bacillus subtilis*. *Mol Gen Genet* **186:** 339–346.

Okubo, S., and Yanagida, T. (1968) Isolation of a suppressor mutant in *Bacillus subtilis*. *J Bacteriol* **95:** 1187–1188.

Orlova, E.V., Gowen, B., Dröge, A., Stiege, A., Weise, F., Lurz, R., *et al*. (2003) Structure of a viral DNA gatekeeper at 10 Å resolution by cryo-electron microscopy. *EMBO J* **22:** 1255–1262.

Parker, M.L., and Eiserling, F.A. (1983) Bacteriophage SPO1 structure and morphogenesis. I. Tail structure and length regulation. *J Virol* **46:** 239–249.

Pell, L.G., Liu, A., Edmonds, L., Donaldson, L.W., Howell, P.L., and Davidson, A.R. (2009) The X-ray crystal structure of the phage lambda tail terminator protein reveals the biologically relevant hexameric ring structure and demonstrates a conserved mechanism of tail termination among diverse long-tailed phages. *J Mol Biol* **389:** 938–951.

Plisson, C., White, H.E., Auzat, I., Zafarani, A., São-José, C., Lhuillier, S., *et al*. (2007) Structure of bacteriophage SPP1 tail reveals trigger for DNA ejection. *EMBO J* **26:** 3720–3728.

Sambrook, J., Fritsh, E.F., and Maniatis, T. (1989) *Molecular Cloning. A Laboratory Manual*. Cold Spring Harbour, NY: Cold Spring Harbor Laboratory Press.

Steven, A.C., Trus, B.L., Maizel, J.V., Unser, M., Parry, D.A.D., Wall, J.S., *et al*. (1988) Molecular substructure of a viral receptor-recognition protein. The gp17 tail-fiber of bacteriophage T7. *J Mol Biol* **200:** 351–365.

Tavares, P., Zinn-Justin, S., and Orlova, E.V. (2012) Genome gating in tailed bacteriophage capsids. *Adv Exp Med Biol* **726:** 585–600.

Tsui, L.C., and Hendrix, R.W. (1983) Proteolytic processing of phage lambda tail protein gpH: timing of the cleavage. *Virology* **125:** 257–264.

Veesler, D., Robin, G., Lichière, J., Auzat, I., Tavares, P., Bron, P., *et al*. (2010) Crystal structure of bacteriophage SPP1 distal tail protein (gp19.1): a baseplate hub paradigm in gram-positive infecting phages. *J Biol Chem* **285:** 36666–36673.

Vianelli, A., Wang, G.R., Gingery, M., Dudz, R.L., Eiserling, F.A., and Goldberg, E.B. (2000) Bacteriophage T4 self-assembly: localization of gp3 and its role in determining tail length. *J Bacteriol* **182:** 680–688.

Vinga, I., Baptista, C., Auzat, I., Petitpas, I., Lurz, R., Tavares, P., *et al*. (2012) Role of bacteriophage SPP1 tail spike protein gp21 on host cell receptor binding and trigger of phage DNA ejection. *Mol Microbiol* **83:** 289–303.

Walker, J.E., Auffret, A.D., Carne, A., Gurnett, A., Hanisch, P., Hill, D., and Saraste, M. (1982) Solid-phase sequence analysis of polypeptides eluted from polyacrylamide gels. An aid to interpretation of DNA sequences exemplified by the *Escherichia coli unc* operon and bacteriophage lambda. *Eur J Biochem* **123:** 253–260.

Yasbin, R.E., Fields, P.I., and Andersen, B.J. (1980) Properties of *Bacillus subtilis* 168 derivatives freed of their natural prophages. *Gene* **12:** 155–159.